

## The Linear Theory of Land and Sea Breeze Circulation

By Hiroshi Niino

*Meteorological Research Institute, 1-1, Nagamine, Yatabe, Tsukuba, Ibaraki 305, JAPAN*  
(Manuscript received 16 June 1987, in revised form 25 August 1987)

### Abstract

The linear theory of land and sea breeze circulation (LSBC) shows that, in the absence of the Coriolis force and under the hydrostatic approximation, there exists a similarity solution. In this solution, the horizontal coordinate is scaled by  $N\kappa^{1/2}\omega_*^{-1/2}$ , the vertical coordinate by  $\kappa^{1/2}\omega_*^{-1/2}$ , the horizontal velocity by  $g\alpha\Delta T/N$ , the vertical velocity by  $g\alpha\Delta T\omega_*/N^2$  and the pressure by  $g\alpha\Delta T\kappa^{1/2}\omega_*^{-1/2}$ , respectively, where  $\omega_*$  and  $\Delta T$  are the frequency and amplitude of the temperature variation at the ground, respectively,  $N$  the Brunt-Väisälä frequency corresponding to the basic density stratification,  $\kappa$  the eddy thermal diffusivity,  $g$  the gravity acceleration and  $\alpha$  the thermal expansion coefficient. The eddy Prandtl number is assumed to be unity.

In the immediate neighborhood of the coastline, a small region in which non-hydrostatic effects are significant and the similarity solution is invalid is present. The horizontal and vertical dimensions of the non-hydrostatic region are of the order of  $(\kappa/N)^{1/2}$  and the vertical velocity becomes of the same order of the horizontal one in this region. Outside of the region, however, the similarity solution remains always valid.

When the Coriolis force is present, the solution outside of the non-hydrostatic region depends only on the non-dimensional Coriolis parameter  $f$  defined by  $f_*/\omega_*$ . If the horizontal dimension  $\lambda_*$  of LSBC is defined by the distance from the coastline at which the non-dimensional velocity of the onshore wind becomes equal to 0.03,  $\lambda_*$  is given by  $\lambda_* = N\kappa^{1/2}\omega_*^{-1/2}F(f)$ , where  $F(f)$  is a universal function of  $f$ .  $F$  remains almost constant (about 2.1) for  $f < 1$  (latitude less than  $30^\circ$ ). When  $f$  becomes larger than 1, however,  $F$  starts to decrease rapidly and becomes equal to 0.9 for  $f=2.0$  (at the Arctic or the Antarctic).

Effects of the eddy Prandtl number and the non-linear process on the flow characteristics are also discussed.

### 1. Introduction

Land and sea breeze circulation (hereafter abbreviated by LSBC) is one of the oldest subjects which have continuously attracted the interest of meteorologists (Rottuno, 1983). There have been extensive observational and numerical studies on LSBC. However, several basic questions concerning the dynamics of LSBC seem not to have been answered yet. The present paper addresses one of these questions, "what determines the horizontal dimension of

LSBC?", in the frame work of a linear theory.

An attempt to study LSBC by means of a linear theory begins with the work of Jeffreys (1922). Since then, a number of works with different interests have contributed to developing the theory. An excellent historical review of these works are given in Rottuno (1983). Here, we will be confined to review only several works which have a direct link with the present study.

It is generally recognized that the factors which affect LSBC are: 1) diurnal variation of the ground temperature, 2) diffusion of heat, 3) static stability, 4) Coriolis force and 5) diffusion of momentum (Kimura and Eguchi, 1978; hereafter referred to as *KE*). The first three

This paper was presented at International Seminar on Studies of Large-Scale Atmospheric Processes by Use of Models (Kyoto, July 1986).

factors are indispensable for producing LSBC. Although the fourth factor is not necessary for producing LSBC, it plays an important role in determining its horizontal dimension and producing the clockwise rotation of the wind vector with time. The fifth factor is not necessary for producing LSBC either. However, it is important for satisfying the no-slip condition at the ground and producing a realistic wind profile near the ground.

A reasonable linear theory which includes all the above five factors was first examined by Walsh (1974). He has shown that the dynamics of LSBC is well described by the hydrostatic equation system. As for the horizontal dimension of LSBC, he mentioned that "... can be said to increase with  $N^2$ . This result suggests an analogy between the circulation's horizontal extent and the Rossby deformation radius  $NH/f_*$ , where  $H$  is the depth of the disturbance". In the above quotation,  $N$  is the Brunt-Väisälä frequency corresponding to the density stratification of the atmosphere, and  $f_*$  the Coriolis parameter. As will be shown later,  $H$  is scaled by the diffusion length  $(\kappa/\omega_*)^{1/2}$ , where  $\omega_*$  is the frequency of the diurnal variation of the ground temperature and  $\kappa$  the eddy thermal diffusion coefficient (or eddy kinematic viscosity  $\nu$  since he assumed that the eddy Prandtl number  $Pr = \nu/\kappa$  is unity). Therefore, the horizontal dimension suggested by Walsh (1974) is equivalent to  $N(\kappa/\omega_*)^{1/2}/f_*$ .

KE considered LSBC over an island of finite width in the absence of the Coriolis force. Assuming that  $Pr$  is unity, they found that the flow field is determined by a single non-dimensional parameter  $\Omega$  defined by  $\Omega = \omega_* (l^2/N^2\kappa)^{1/3}$ , where  $l$  is the width of the island. Furthermore, they showed that, for  $\Omega < 1.3$ , the flow structure is similar to that of the steady heat island ( $\Omega = 0$ ). On the other hand, for  $\Omega > 1.3$ , they suggested that the horizontal dimension of LSBC is mainly determined by the characteristics of the internal gravity wave by comparing their results with those of their inviscid model. However, they did not give an explicit expression for the horizontal dimension.

It is interesting to note that the non-dimensional parameter  $\Omega$  can be written as

$$\Omega = (l/L)^{2/3},$$

where  $L = N\kappa^{1/2}\omega_*^{-3/2}$  has a dimension of length. What does this length scale mean physically? It coincides with the horizontal wavelength of the hydrostatic internal gravity wave whose frequency and vertical scale are  $\omega_*$  and  $(\kappa/\omega_*)^{1/2}$ , respectively. It also coincides with the horizontal distance to which the same internal gravity wave can transport its energy from the coastline within a day ( $\sim \omega_*^{-1}$ ). Thus, if the horizontal dimension of LSBC would be determined by the dynamics of the internal gravity wave as suggested by KE, it should have a close relationship to the length scale  $L$ .

Ueda (1983) extended the work of Walsh (1974) to the case in which  $Pr$  is not equal to unity, and also examined the structure of a steady convection for which  $\omega_* = 0$  and  $f_* \neq 0$ . He obtained an experimental formula that the horizontal dimension of LSBC was proportional to

$$(N/\omega_*)^{0.774} (\nu/\omega_*)^{1/2} Pr^0. \quad (1.3)$$

He also found that the Coriolis force did not affect the horizontal dimension of LSBC.

Rottuno (1983) considered an inviscid model of LSBC in which a thermal forcing is present above the coastline. He showed that the nature of the response of the inviscid atmosphere changes markedly according to whether  $f_*$  is larger than  $\omega_*$  or less, where  $\omega_*$  is to be understood as the forcing frequency. Especially he suggested that the horizontal dimension of LSBC is given by  $Nh(\omega_*^2 - f_*^2)^{-1/2}$  for  $f_* < \omega_*$  and by  $Nh(f_*^2 - \omega_*^2)^{-1/2}$  for  $f_* > \omega_*$ , where  $h$  is the vertical scale of the thermal forcing and may be regarded as the diffusion length  $(\kappa/\omega_*)^{1/2}$  for the present purpose. If KE's work is interpreted as suggesting that the horizontal dimension of LSBC is given by  $L = N\kappa^{1/2}\omega_*^{-3/2}$  as discussed above, Rottuno's work can be regarded as an extension of KE's idea to a rotating system.

We have reviewed several recent works which study the linear dynamics of LSBC. Even if we are confined to these works, there exist three different expressions for the horizontal dimension of LSBC. Which expression is the correct one? Where do such contradictions originate from? It is the purpose of the present paper

to provide definite answers to these questions.

In the following section, the problem is formulated. The non-dimensionalization of the governing equations and the boundary conditions form the kernel of the present analysis. The results are shown in Section 3 and are discussed in the light of the previous studies in Section 4. They are summarized in the last section.

2. Formulation of the problem

2.1. Model

Consider a straight coastline as shown in Fig. 1. The  $x_*$ - and  $y_*$ -axes are taken to the horizontal directions perpendicular to and along the coastline, respectively, and the  $z_*$ -axis to the vertical direction. The land occupies the right half of the earth's surface ( $x_* > 0$ ), while the sea the left half ( $x_* < 0$ ). The whole system is rotating about the vertical axis at a constant angular velocity  $f_*/2$ .

The atmosphere in the basic state is assumed to be motionless and have a constant positive vertical temperature<sup>1)</sup> gradient  $\Gamma$ , so that the temperature  $\bar{T}_*$  in the basic state is given by

$$\bar{T}_* = T_{0*} + \Gamma z_*, \tag{2.1}$$

where  $T_{0*}$  is the temperature at the earth's surface ( $z_* = 0$ ) in the basic state.

The temperature  $T_{L*}$  on the land surface is assumed to change periodically with time around its mean value with the amplitude  $\Delta T_*$  and the frequency  $\omega_*$ , so that it is given by

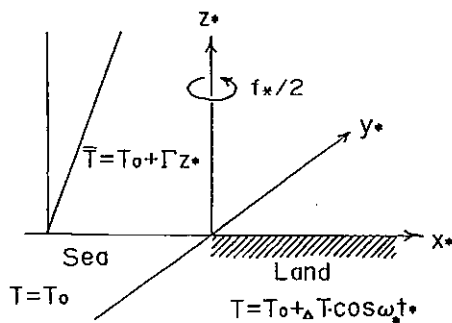


Fig. 1. Schematic diagram of the model.

<sup>1)</sup> Strictly speaking, the word "temperature" should be hereafter replaced by "potential temperature".

$$T_{L*} = T_{0*} + \Delta T_* \cos \omega_* t_* \quad (x_* > 0), \tag{2.2}$$

where  $t_*$  is time. On the other hand, the temperature  $T_{S*}$  on the sea surface is assumed to remain constant with time;

$$T_{S*} = T_{0*} \quad (x_* < 0). \tag{2.3}$$

It is the purpose of this paper to examine the response of the viscous stratified fluid to the differential heating given by (2.2) and (2.3). Since the vertical dimension of LSBC is expected to be small compared with the scale height of the atmosphere, the atmosphere may be regarded as a Boussinesq fluid.

2.2. Governing equations and non-dimensionalization

If the response of the atmosphere is assumed to be uniform in the alongshore direction ( $\partial/\partial y_* = 0$ ), the governing equations in the non-dimensional form are given by

$$\begin{aligned} \frac{\partial u}{\partial t} + \epsilon \left( u \frac{\partial u}{\partial x} + w \frac{\partial u}{\partial z} \right) - f v \\ = - \frac{\partial p}{\partial x} + Pr \left( \delta^2 \frac{\partial^2 u}{\partial x^2} + \frac{\partial^2 u}{\partial z^2} \right), \end{aligned} \tag{2.4}$$

$$\begin{aligned} \frac{\partial v}{\partial t} + \epsilon \left( u \frac{\partial v}{\partial x} + w \frac{\partial v}{\partial z} \right) + f u \\ = Pr \left( \delta^2 \frac{\partial^2 v}{\partial x^2} + \frac{\partial^2 v}{\partial z^2} \right), \end{aligned} \tag{2.5}$$

$$\begin{aligned} \delta^2 \left[ \frac{\partial w}{\partial t} + \epsilon \left( u \frac{\partial w}{\partial x} + w \frac{\partial w}{\partial z} \right) \right] \\ = - \frac{\partial p}{\partial z} + T + Pr \delta^2 \left[ \delta^2 \frac{\partial^2 w}{\partial x^2} + \frac{\partial^2 w}{\partial z^2} \right], \end{aligned} \tag{2.6}$$

$$\begin{aligned} \frac{\partial T}{\partial t} + \epsilon \left( u \frac{\partial T}{\partial x} + w \frac{\partial T}{\partial z} \right) + w \\ = \delta^2 \frac{\partial^2 T}{\partial x^2} + \frac{\partial^2 T}{\partial z^2}, \end{aligned} \tag{2.7}$$

$$\frac{\partial u}{\partial x} + \frac{\partial w}{\partial z} = 0, \tag{2.8}$$

where the following non-dimensionalizations are introduced:

$$t_* = \omega_*^{-1} t, \quad x_* = \frac{N}{\omega_*} \left( \frac{\kappa}{\omega_*} \right)^{1/2} x,$$

$$\begin{aligned}
 z_* &= \left(\frac{\kappa}{\omega_*}\right)^{1/2} z, \quad (u_*, v_*) = \frac{g\alpha\Delta T_*}{N} (u, v), \\
 w_* &= \frac{\omega_*}{N} \frac{g\alpha\Delta T_*}{N} w, \quad p_* = g\alpha\Delta T_* \left(\frac{\kappa}{\omega_*}\right)^{1/2} p, \\
 T'_* &= \Delta T_* \cdot T, \quad f_* = \omega_* \cdot f. \quad (2.9)
 \end{aligned}$$

$u_*, v_*$  and  $w_*$  are the velocity components in the  $x_*$ ,  $y_*$  and  $z_*$ -directions, respectively,  $T'_*$  deviation of the total temperature  $T_*$  from the basic state temperature  $\bar{T}_*$  ( $T'_* = T_* - \bar{T}_*$ ),  $p_*$  the kinematic pressure and  $g$  the gravity acceleration. The Coriolis parameter  $f_*$  is given by  $f_* = 2\omega_* \sin \phi$ , where  $\phi$  is the latitude. The Brunt-Väisälä frequency  $N$  is defined by  $N = (g\alpha\Gamma)^{1/2}$ , where  $\alpha = 1/T_{v*}$  is the volume expansion coefficient.

The boundary conditions at the earth's surface are assumed to be such that all the velocity components vanish and the temperature be given by (2.2) and (2.3); i.e.,

$$\begin{aligned}
 u = v = w = 0 \text{ and} \\
 T = \begin{cases} \cos t & \text{for } x > 0 \\ 0 & \text{for } x < 0 \end{cases} \text{ at } z = 0. \quad (2.10)
 \end{aligned}$$

It is also required that  $u, v, w$  and  $T$  vanish at  $z = \infty$ .

The equations (2.4) – (2.8) and the boundary conditions (2.10) contain four non-dimensional parameters  $f, \delta, Pr$  and  $\epsilon$ .  $f = 2 \sin \phi$  is the non-dimensional Coriolis parameter,  $Pr = \nu/\kappa$  the eddy Prandtl number and  $|\delta| = \omega_*/N$  the ratio of the frequency of the temperature variation of the ground to the Brunt-Väisälä frequency.  $\epsilon = \Delta T_* / [T(\kappa/\omega_*)^{1/2}]$  is the ratio of the amplitude of the temperature change at the earth's surface to the vertical temperature difference in the basic state over the diffusion length, and measures the importance of the nonlinear effects relative to the linear ones.

For typical atmospheric conditions,  $\omega_* \sim 10^{-4} \text{ s}^{-1}$ ,  $N \sim 10^{-2} \text{ s}^{-1}$ ,  $\nu \sim \kappa \sim 10 \text{ m}^2 \text{ s}^{-1}$  and  $\Delta T \sim 5^\circ \text{ K}$ , so that  $\epsilon \sim 10$ ,  $Pr \sim 1$  and  $\delta \sim 10^{-2}$ . The value of  $f$  changes from 0 to 2 as the latitude moves from  $0^\circ$  to  $90^\circ$ .

Since  $\delta$  is regarded as an aspect ratio (see, (2.9)), the smallness of  $\delta$  suggests that the hydrostatic approximation ( $\delta = 0$ ) will be excel-

lent (cf. Walsh, 1974) except near the coastline where the horizontal temperature gradient may become large (see Section 3).

The value of  $Pr$  is expected to be of the order of one, but its exact value has not been determined either observationally nor theoretically. Therefore, we will hereafter assume that  $Pr$  is equal to 1 for simplicity. The effect of  $Pr$  will be discussed in Section 4.

Although the above estimate of  $\epsilon$  suggests that the nonlinear effects can be important for LSBC observed in nature, we will hereafter be concerned with the linear theory in which  $\epsilon \ll 1$  is assumed. The effects of nonlinearity will be briefly discussed in Section 4.

Under the assumptions  $\epsilon \ll 1$  and  $Pr = 1$ , the governing equations (2.4) – (2.7) are reduced to

$$\frac{\partial u}{\partial t} - f v = -\frac{\partial p}{\partial x} + \delta^2 \frac{\partial^2 u}{\partial x^2} + \frac{\partial^2 u}{\partial z^2}, \quad (2.11)$$

$$\frac{\partial v}{\partial t} + f u = \delta^2 \frac{\partial^2 v}{\partial x^2} + \frac{\partial^2 v}{\partial z^2}, \quad (2.12)$$

$$\delta^2 \frac{\partial w}{\partial t} = -\frac{\partial p}{\partial z} + T + \delta^2 \left( \delta^2 \frac{\partial^2 w}{\partial x^2} + \frac{\partial^2 w}{\partial z^2} \right), \quad (2.13)$$

$$\frac{\partial T}{\partial t} + w = \delta^2 \frac{\partial^2 T}{\partial x^2} + \frac{\partial^2 T}{\partial z^2}, \quad (2.14)$$

These equations together with (2.8) and (2.10) constitute the problem to be solved in the following.

Before solving the problem for a general case in which  $f \neq 0$  and  $\delta \neq 0$ , we will first consider the simplest case  $f = \delta = 0$  (i.e., the Coriolis force is absent and the hydrostatic approximation is made). It is easily observed that, in this case, the problem becomes independent of any external parameters. This means that there exists a similarity solution for this problem. Once the solution, say  $u = u(x, z, t)$ , is known, the dimensional solution  $u^*$  can be expressed as

$$\begin{aligned}
 u_* = \frac{g\alpha\Delta T_*}{N} u \left( \frac{\omega_*}{N} \left( \frac{\omega_*}{\kappa} \right)^{1/2} x_*, \right. \\
 \left. \left( \frac{\omega_*}{\kappa} \right)^{1/2} z_*, \omega_* t_* \right). \quad (2.15)
 \end{aligned}$$

Thus, the horizontal dimension  $\lambda_*$  of LSBC should be scaled by

$$\frac{N}{\omega_*} \left( \frac{\kappa_*}{\omega_*} \right)^{1/2}$$

When  $\delta=0$  but  $f \neq 0$ , the solution will depend on  $f$ . Therefore,  $\lambda_*$  will be given by

$$\lambda_* = \frac{N}{\omega_*} \left( \frac{\kappa}{\omega_*} \right)^{1/2} F(f), \tag{2.16}$$

where  $F(f)$  is a universal function of  $f$ .

Since the value of  $\delta$  in the atmosphere is very small, the solution for the general case is expected to deviate little from the hydrostatic solution. Thus, the above deductions concerning the horizontal dimension of LSBC are likely to remain valid for  $\delta \neq 0$  as far as the condition  $\delta \ll 1$  is satisfied.

If any variable, say  $\eta(x, z, t)$ , is expressed as  $\eta = \text{Re}[\hat{\eta}(x, z)e^{it}]$  and this expression is substituted into the governing equations, we obtain equations for the amplitude  $\hat{\eta}$ , where  $\text{Re}$  denotes the real part of the quantity in the bracket. If these equations are used to derive a single equation for  $\hat{T}$ , we have

$$\left\{ \left[ \left( i - \delta^2 \frac{\partial^2}{\partial x^2} - \frac{\partial^2}{\partial z^2} \right)^2 + f^2 \right] \frac{\partial^2}{\partial z^2} + \left[ \delta^2 \left( i - \delta^2 \frac{\partial^2}{\partial x^2} - \frac{\partial^2}{\partial z^2} \right)^2 + 1 \right] \frac{\partial^2}{\partial x^2} \right\} \cdot \left( \delta^2 \frac{\partial^2}{\partial x^2} + \frac{\partial^2}{\partial z^2} - i \right) \hat{T} = 0. \tag{2.17}$$

If the hydrostatic approximation ( $\delta=0$ ) is made, eq. (2.17) becomes

$$\left\{ \left[ \left( i - \frac{\partial^2}{\partial z^2} \right)^2 + f^2 \right] \frac{\partial^2}{\partial z^2} + \frac{\partial^2}{\partial x^2} \right\} \cdot \left( \frac{\partial^2}{\partial z^2} - i \right) \hat{T} = 0. \tag{2.18}$$

Since the boundary condition for  $\hat{T}$  at  $z=0$  becomes

$$\hat{T} = \begin{cases} 1 & \text{for } x > 0 \\ 0 & \text{for } x < 0, \end{cases} \tag{2.19}$$

$\partial \hat{T} / \partial x$  becomes infinite as  $x \rightarrow 0$  and  $z \rightarrow 0$ . In order that eq. (2.18) is satisfied, this means that  $\partial \hat{T} / \partial z$  must also become infinite as  $x \rightarrow 0$  and

$z \rightarrow 0$ . Thus, near the coastline, eq. (2.18) becomes approximately

$$\left( \frac{\partial^6}{\partial z^6} + \frac{\partial^2}{\partial x^2} \right) \frac{\partial^2}{\partial z^2} T = 0, \tag{2.20}$$

which implies that, for  $x \sim O(\mu)$  ( $\mu \ll 1$ ),  $\partial \hat{T} / \partial x$  becomes  $O(\mu^{-1})$ , while  $\partial \hat{T} / \partial z$  becomes  $O(\mu^{-1/2})$ . Now, an inspection of eq. (2.17) shows that, when  $x$  becomes  $O(\delta^{3/2})$ , the non-hydrostatic terms, which are multiplied by  $\delta^2$ , become important. For  $x \sim O(\delta^{3/2})$  and  $z \sim O(\delta^{1/2})$ , the governing equations (2.11) – (2.14) and (2.8) become

$$0 = -\frac{\partial \hat{p}}{\partial x} + \delta^2 \frac{\partial^2 \hat{u}}{\partial x^2} + \frac{\partial^2 \hat{u}}{\partial z^2}, \tag{2.21}$$

$$0 = \delta^2 \frac{\partial^2 \hat{v}}{\partial x^2} + \frac{\partial^2 \hat{v}}{\partial z^2}, \tag{2.22}$$

$$0 = -\frac{\partial \hat{p}}{\partial z} + \hat{T} + \delta^2 \left( \delta^2 \frac{\partial^2 \hat{w}}{\partial x^2} + \frac{\partial^2 \hat{w}}{\partial z^2} \right), \tag{2.23}$$

$$\hat{w} = \delta^2 \frac{\partial^2 \hat{T}}{\partial x^2} + \frac{\partial^2 \hat{T}}{\partial z^2}, \tag{2.24}$$

$$\frac{\partial \hat{u}}{\partial x} + \frac{\partial \hat{w}}{\partial z} = 0. \tag{2.25}$$

Assuming that  $\hat{T} \sim O(1)$ ,  $\partial / \partial x \sim O(\delta^{-3/2})$  and  $\partial / \partial z \sim O(\delta^{-1/2})$ , we can derive from eqs. (2.21) – (2.25) that  $\hat{w} \sim O(\delta^{-1})$ ,  $\hat{u} \sim O(1)$  and  $\hat{p} \sim O(\delta^{1/2})$ . Thus, in the region whose horizontal and vertical dimensions are  $O(\delta^{3/2})$  and  $O(\delta^{1/2})$ , respectively (in dimensional units, both are  $O((\kappa/N)^{1/2})$ ), the vertical velocity becomes large and of the order of  $\delta^{-1}$  (in dimensional unit, this

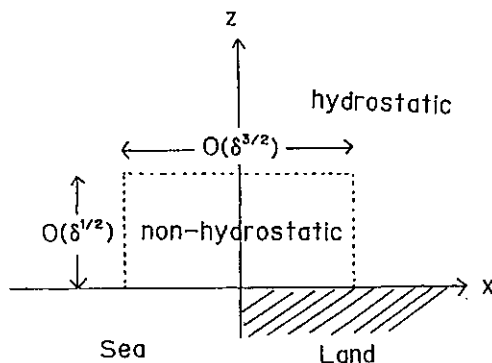


Fig. 2. Flow structure near the coastline.

is of the same order of the horizontal velocity). The region is hereafter called the non-hydrostatic region (see Fig. 2). It is noted that the equations (2.21) – (2.25) do not contain the terms of time rate of change nor the Coriolis terms. Thus the structure of the non-hydrostatic region does not explicitly depend on the effects of time change and Coriolis force.

### 2.3. Method of solution

The method of solution is same as in the previous works (Walsh(1974), KE, and Ueda (1983)). The equations for the amplitude  $\hat{\eta}(x, z)$  are Fourier-transformed in the horizontal direction, then solved in the vertical direction, and finally, inversely Fourier-transformed to obtain the solution for the amplitude.

The evaluation of the inverse Fourier-transformation with respect to the wavenumber  $k$  in the  $x$ -direction has to rely on numerical calculations which utilize the Newton's integration formula. Two calculations have been made with different independent variables. One approximates the integration for  $-\infty < k < +\infty$  by that for  $-200 < k < 200$  with independent variable  $k$  and grid interval  $\Delta k = 0.01$ . The other approximates the same integration by that for  $-10^5 < k < 10^5$  with independent variable  $K = 200 + 199.99(\log|k| - 5.8)/8.0$  and grid interval  $\Delta K = 0.01$ . The latter calculation is found to have enough resolution to obtain the accurate flow structure in the non-hydrostatic region. On the other hand, outside of the non-hydrostatic region the flow structures obtained by the two calculation essentially coincide with each other.

## 3. Results

### 3.1. Non-hydrostatic effect

In order to see the effect of hydrostatic approximation on the flow field, we first examine the results for various values of  $\delta$ . The Coriolis force is not considered for simplicity throughout this subsection.

Fig. 3 shows the absolute value of the amplitude of the horizontal wind,  $|\hat{u}(x, z)|$  for  $\delta = 0$  and  $10^{-1}$ . Note that  $|\hat{u}(-x, z)| = |\hat{u}(x, z)|$ . The overall pattern of  $|\hat{u}|$  remains similar for  $0 \leq \delta < 10^{-1}$ . Near the coastline where the non-hydrostatic region is expected, however, the

pattern of  $|\hat{u}|$  seems to changes with  $\delta$ . (Note that the horizontal and vertical dimensions of the non-hydrostatic region in Fig. 3(b) are of the order of 0.03 and 0.3, respectively.)

Fig. 4 which shows the vertical profile of  $|\hat{u}|$  at  $x=0$  illustrates more clearly the change of the pattern of  $|\hat{u}|$  with  $\delta$ . As  $\delta$  is decreased, the maximum value of  $|\hat{u}|$  increases and the height at which  $|\hat{u}|$  becomes maximum decreases. These features seem to support the presence of the non-hydrostatic region as suggested in the previous section. In Fig. 4 the profile for  $\delta=0$  for  $z < 10^{-1}$  may not be reliable, because our numerical calculations do not have enough resolution of the flow fields for  $z < 10^{-1}$ .<sup>2)</sup>

Fig. 5 shows close-up views of  $|\hat{w}|$  near the coastline for  $\delta=0.01$  and  $\delta=0.02$ . For these values of  $\delta$ , the horizontal and vertical dimensions of the non-hydrostatic region are of the order of  $10^{-3}$  and  $10^{-1}$ , respectively. It is seen that, for larger value of  $\delta$ , the maximum value of  $|\hat{w}|$ ,  $w_{\max}$ , is smaller and the values of  $x$  and  $z$  at which  $|\hat{w}|$  becomes maximum,  $x_{\max}$  and  $z_{\max}$ , are larger. It is also noted that  $|\hat{w}|$  decreases rapidly with  $x$  as  $x$  is increased from  $x_{\max}$ .

Fig. 6 summarizes the values of  $\hat{w}_{\max}$ ,  $x_{\max}$ ,  $z_{\max}$  obtained for various values of  $\delta$ . The dots show the results of the numerical calculations, and the straight lines the theoretical prediction for the non-hydrostatic region that  $\hat{w}_{\max} \sim \delta^{-1}$ ,  $x_{\max} \sim \delta^{3/2}$  and  $z_{\max} \sim \delta^{1/2}$ . Each of the results of the numerical calculations fits the corresponding theoretical prediction very well.

In summary, the flow structure outside of the non-hydrostatic region near the coastline does not depend on  $\delta$  and is essentially the same as that of the hydrostatic solution ( $\delta=0$ ) as far as  $\delta < 10^{-1}$  is satisfied. Although the results in the case of the presence of Coriolis

<sup>2)</sup> In the non-hydrostatic region, the vertical wavenumber characteristic of a phenomenon whose characteristic horizontal wavenumber is  $k$  is of the order of  $k^{1/3}$  (see, eq. (2.20)). Since the largest horizontal wavenumber considered in the present numerical calculation is  $10^5$ , the corresponding largest vertical wavenumber is  $10^{5/3}$ . This means that the smallest vertical scale that can be resolved in the present calculation is  $2\pi/10^{5/3} \sim 0.13$ .

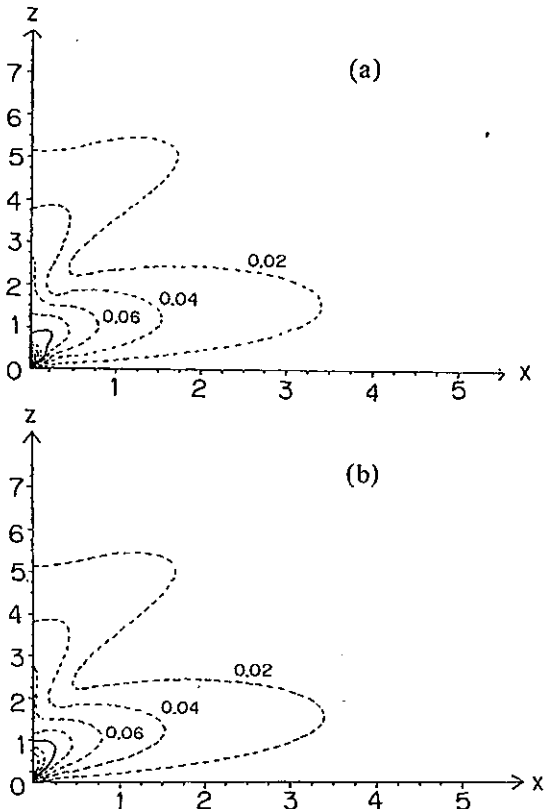


Fig. 3. Distribution of absolute value of the amplitude of the horizontal wind  $|\hat{u}(x, z)|$  for (a)  $\delta = 0$  and (b)  $\delta = 10^{-1}$ . Only the distribution for  $x > 0$  is shown, since  $|\hat{u}(-x, z)| = |\hat{u}(x, z)|$ . Dashed contour lines are drawn for each 0.02, and solid ones for each 0.1.

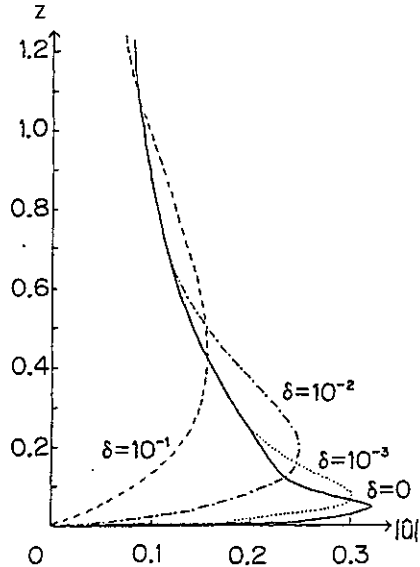


Fig. 4. Vertical profile of  $|\hat{u}|$  above the coastline for various values of  $\delta$  ( $\delta = 0, 10^{-3}, 10^{-2}$  and  $10^{-1}$ ).

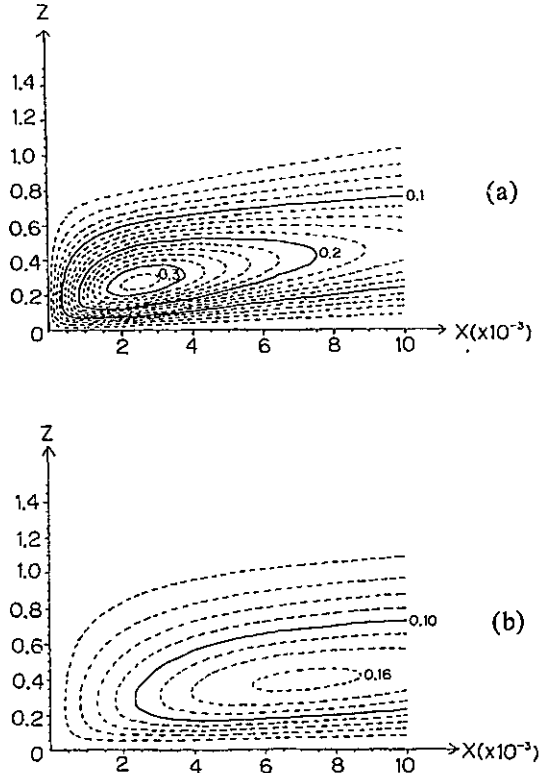


Fig. 5. Distribution of  $|\hat{w}(x, z)|$  near the coastline for (a)  $\delta = 0.01$  and (b)  $\delta = 0.02$ . Notice that the unit of the horizontal axis is  $10^{-3}$ . Dashed contour lines are drawn for each 0.02, and solid ones for each 0.1.

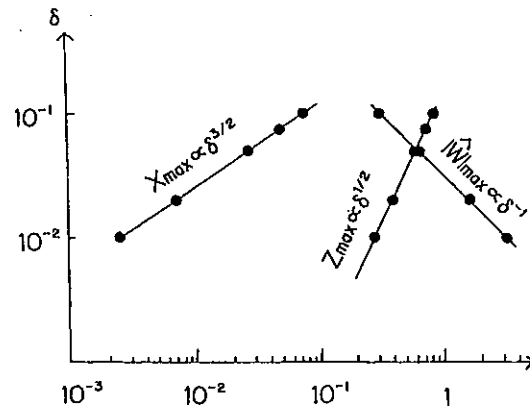


Fig. 6. Comparison of the calculated values of  $\hat{w}_{\max}$ ,  $x_{\max}$ ,  $z_{\max}$  with the theoretical predictions.

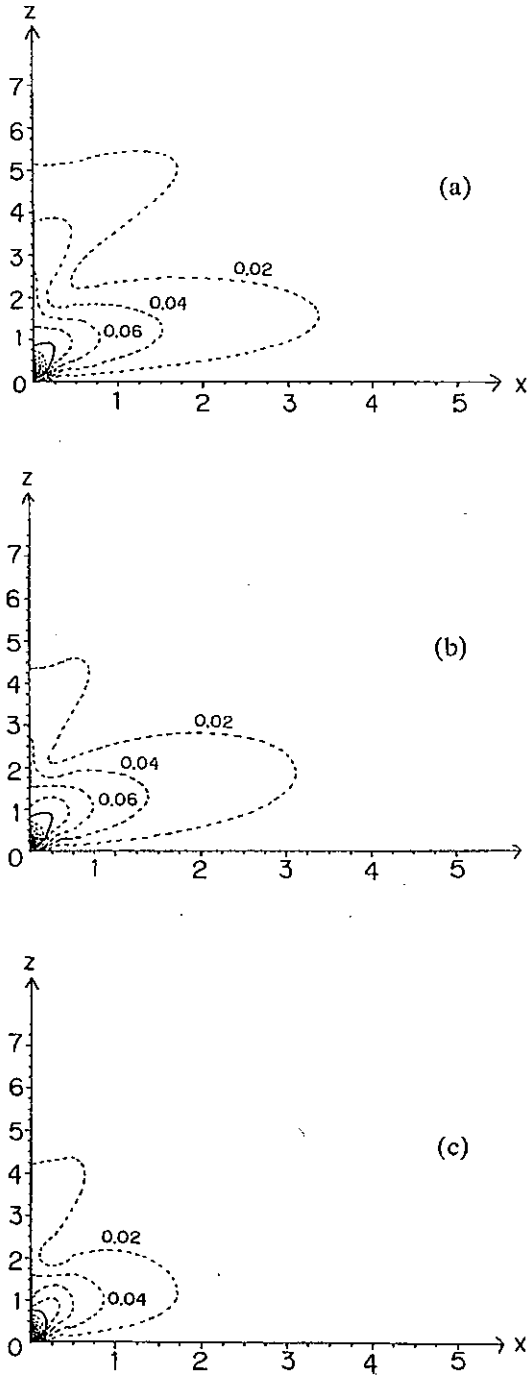


Fig. 7. Distribution of absolute value of the amplitude of the horizontal wind  $|\hat{u}(x, z)|$  for various values of  $f$  ((a)  $f = 0$ , (b)  $f = 1.0$  and (c)  $f = 1.5$ ). Dashed contour lines are drawn for each 0.02, and solid ones for each 0.1.

force are not shown, the effects of  $\delta$  on the flow structure are expected to remain quite similar, since eqs. (2.21) – (2.25) suggest that the structure of the non-hydrostatic region does not depend on the Coriolis parameter explicitly.

### 3.2 Effect of the Coriolis force

Fig. 7 shows the pattern of  $|\hat{u}|$  for various values of the non-dimensional Coriolis parameter  $f$ . Since the solution outside the non-hydrostatic region does not depend on  $\delta$  for  $\delta < 10^{-1}$ ,  $\delta$  is fixed to  $10^{-2}$  throughout this subsection. It is seen from Fig. 7 that the pattern of  $|\hat{u}|$  remains similar for  $f < 1.0$ , but it starts to change rapidly as  $f$  becomes larger than 1.0.

Fig. 7 also shows that, for a fixed value of  $x$ ,  $|\hat{u}|$  has two peaks in the vertical direction. The peak near the ground corresponds to the sea or land breeze, and the other peak at higher altitude to its compensating flow. If the peak values near the ground and at higher altitude for a fixed value of  $x$  are denoted by  $|u_{SL}|$  and  $|u_C|$ , respectively,  $|u_{SL}|$  is always larger than  $|u_C|$ . Fig. 8 shows the dependence of  $|u_{SL}|$  on the distance from the coastline for several values of  $f$ . It is seen that the offshore or onshore wind decreases in amplitude rapidly with increasing  $x$ . It is also seen that the dependence of  $|u_{SL}|$  on  $x$  remains similar for  $f < 1.0$ . For  $f > 1.0$ , however,  $|u_{SL}|$  decreases markedly with increasing  $f$  for all  $x$ .

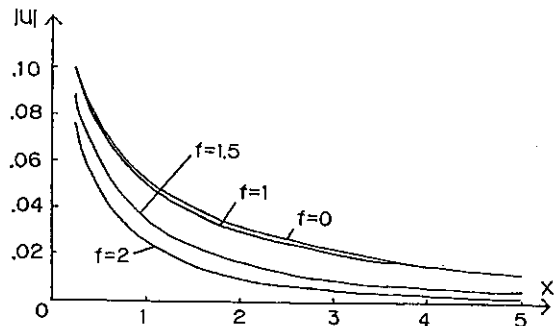


Fig. 8. Dependence of  $|u_{SL}|$  on the distance from the coastline.

Fig. 9 shows the non-dimensional horizontal dimension  $\lambda$  ( $= F(f)$  in (2.16)) as a function of  $f$  when  $\lambda$  is defined by the value of  $x$  for which  $|u_{SL}|$  becomes equal to  $0.03^3$ . For

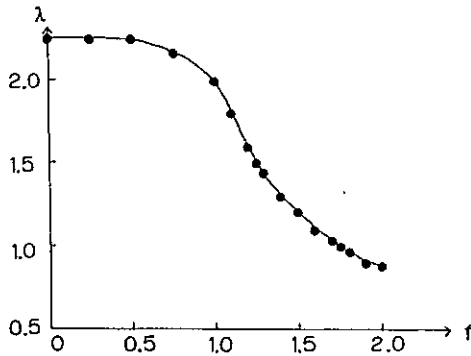


Fig. 9. Dependence of the non-dimensional horizontal dimension  $\lambda$  of LSBC on the non-dimensional Coriolis parameter  $f$

typical atmospheric conditions ( $N \sim 10^{-2} s^{-1}$ ,  $T_{0*} \sim 300^\circ K$ ,  $\Delta T \sim 5^\circ K$ ), this corresponds to 0.5m/s. It is seen from Fig. 9 that  $\lambda$  remains almost constant (2.0~2.2) for  $f < 1.0$ . As  $f$  is increased from 1.0, however,  $\lambda$  decreases rapidly with  $f$  and becomes about 0.9 for  $f=2.0$ . This means that, even if same external parameters are imposed, the horizontal dimension of LSBC at the poles is less than half of that at the equator because of the effect of the Coriolis force. It is also noted that the effect of the Coriolis force becomes significant only when the latitude is larger than  $30^\circ$ .

3.3 Time evolution

Fig. 10 shows time evolution of LSBC for  $\delta=10^{-2}$  and  $f=0$ . The flow fields are shown only for the half period ( $-\pi/2 < t < \pi/2$ ). Note that

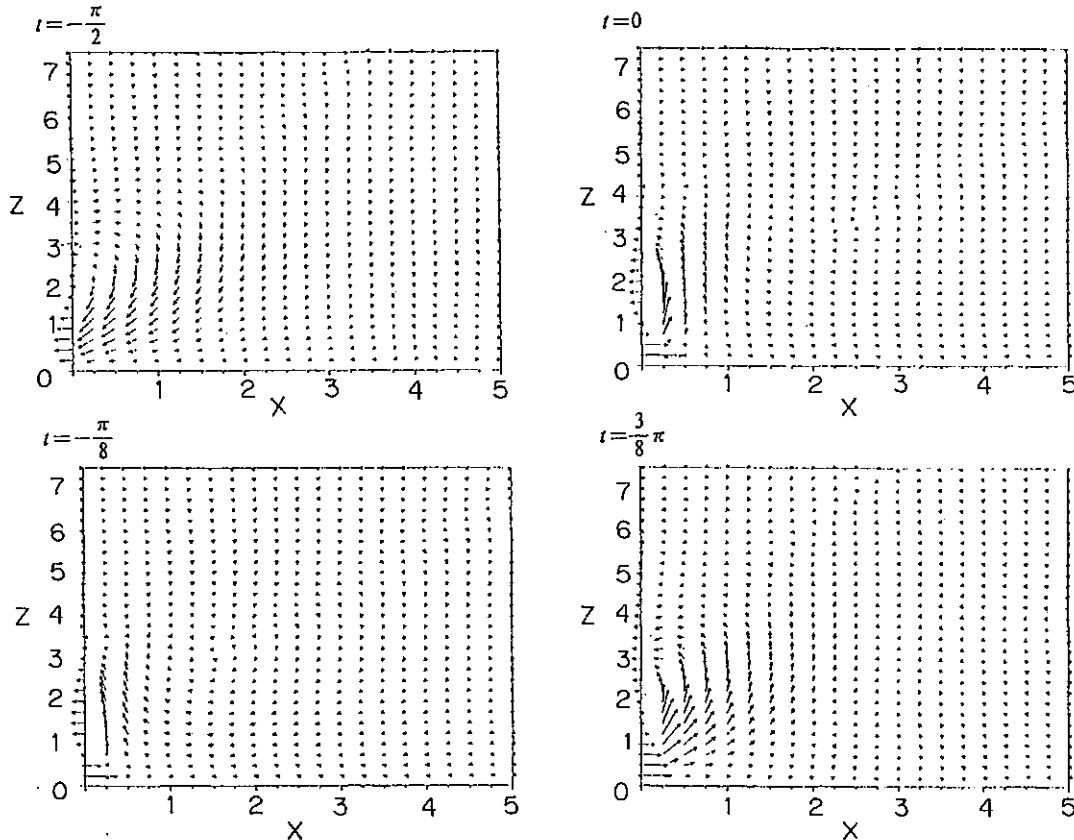


Fig. 10. Time evolution of LSBC for  $\delta=10^{-2}$  and  $f=0$ .

3) The choice of this particular value was made rather arbitrarily. If the value is doubled (i.e., 0.06), the horizontal dimension  $\lambda$  becomes about one third of the value shown in Fig. 9.

the temperature perturbation at the ground varies as  $\cos(t)$ .

At  $t=-\pi/2$  when the temperature perturbation

at the ground vanishes, the land breeze is still dominant near the earth's surface. As the temperature perturbation increases, the sea breeze is initiated near the surface of the coastline and gradually increases its strength. However, the sea breeze is confined to the neighbourhood of the coastline (say,  $x < 0.25$ ) even at  $t = \pi/8$ . Thus, there is a strong convergence and upward motion around  $x = 0.25$ .

At  $t = 0$  when the temperature perturbation attains its maximum value, the sea breeze intrudes to  $x = 0.25$ . It is interesting to note that the height of the maximum horizontal velocity at  $x = 0.25$  is around  $z = 0.75$ , while that at  $x = 0$  is close to the earth's surface. This is because there is the non-hydrostatic region at  $x = 0$  (see, Fig. 4). The sea breeze continues to strengthen and intrude inland until  $t = \pi/2$  at which the temperature perturbation vanishes again (see,  $t = -\pi/2$ ). From  $t = 0$  to  $t = \pi/2$ , the height at which the horizontal velocity becomes maximum is almost unchanged for  $x < 1.0$  and is between 0.75 and 1.25, although it seems to increase slightly with  $x$  for  $x > 1.0$ . After  $t = \pi/2$  the land breeze starts to develop on the coastline. The time evolution of the land breeze is the same as that of the sea breeze except that the flow direction is opposite.

#### 4. Discussion of the results

##### 4.1 Comparison with the previous studies

The main results obtained in the previous section may be summarized as follows:

- (1) LSBC is well described by the hydrostatic equation system ( $\delta = 0$ ) except in the non-hydrostatic region near the coastline, and the flow fields outside of the non-hydrostatic region for  $\delta \neq 0$  coincide with those of the hydrostatic solution as far as  $\delta = \omega_*/N < 10^{-1}$  is satisfied.
- (2) The horizontal dimension of LSBC,  $\lambda_*$ , is scaled by  $(N/\omega)(\kappa/\omega_*)^{1/2}$ , and can be expressed as

$$\lambda_* = \frac{N}{\omega_*} \left( \frac{\kappa}{\omega_*} \right)^{1/2} \cdot F(f), \quad (4.1)$$

where  $F(f)$  is a function of the non-dimensional Coriolis parameter  $f = f_*/\omega_*$ .  $F(f)$  remains constant ( $\sim 2.1$ ) for  $f < 1.0$ , but monotonically decreases with increasing  $f$  for  $f > 1.0$  and be-

comes 0.9 for  $f = 2.0$ .

On the other hand, the main results of the previous studies reviewed in the introduction are summarized in Table 1.

The fact that LSBC is well described by the hydrostatic equation system was shown by Walsh (1974) for several particular combinations of the external parameters. Since he introduced a wrong scaling of variables such that the horizontal and the vertical coordinates are scaled by the diffusion length, however, he was not able to prove the fact for a general case. Furthermore, he did not notice the presence of the non-hydrostatic region above the coastline. As for the horizontal dimension  $\lambda_*$ , he suggested the following relation

$$\lambda_* \sim (N/f_*)(\kappa/\omega_*)^{1/2}. \quad (4.2)$$

However, this relation predicts  $\lambda_* \rightarrow \infty$  as  $f_* \rightarrow 0$ . Since the presence of the Coriolis force is not essential for producing LSBC,  $\lambda_*$  should be defined even for  $f_* = 0$  (see, eq. (4.1)). Thus, eq. (4.2) is considered to be incorrect. It is important to point out that, if his Figs. 2, 3, 4 and 5 are simply re-scaled according to (2.9), they would include more general cases (for a fixed value of  $f$ ) except for several features associated with the non-hydrostatic layer in the immediate neighbourhood of the coastline.

KE and Rottuno (1983) argued that  $\lambda_*$  is determined by the inviscid dynamics. Especially, Rottuno (1983) suggested that  $\lambda_*$  is given by

$$\frac{N}{(\omega_*^2 - f_*^2)^{1/2}} \left( \frac{\kappa}{\omega_*} \right)^{1/2} \quad \text{for } \omega_* > f_* (\phi < 30^\circ)$$

$$\frac{N}{(f_*^2 - \omega_*^2)^{1/2}} \left( \frac{\kappa}{\omega_*} \right)^{1/2} \quad \text{for } \omega_* < f_* (\phi > 30^\circ)$$
(4.3)

However, this expression shows that  $\lambda_* \rightarrow \infty$  at the inertial latitude ( $\omega_* = f_*$ ). Rottuno (1983) argued that the effect of viscosity must become important for  $\omega_* = f_*$ . However, there seems to be no particular reason that the viscosity is important only for the case of  $\omega_* = f_*$ . Equations (2.4) and (2.5) show that the magnitude of the vertical diffusion term in the horizontal momentum equation is of the same order as that of the

Table 1. Comparison of the present results with those of the previous studies.

	Model	Scaling	Horizontal scale $\lambda_*$	Definition of $\lambda$	Comments
Walsh (1974)	<ul style="list-style-type: none"> <li>• non-hydrostatic</li> <li>• <math>f \neq 0</math></li> <li>• <math>Pr=1</math></li> </ul>	$\begin{pmatrix} x_* \\ z_* \end{pmatrix} = \sqrt{\frac{\kappa}{\omega_*}} \begin{pmatrix} x \\ z \end{pmatrix}$ $\begin{pmatrix} u_* \\ v_* \\ w_* \end{pmatrix} = \frac{g\alpha\Delta T_*}{\omega_*} \begin{pmatrix} u \\ v \\ w \end{pmatrix}$	$\frac{N}{f_*} \sqrt{\frac{\kappa}{\omega_*}}$	value of $x$ at which $u=0$ for fixed $z$ and $t$	non-hydrostatic effects are not important.
Kimura & Eguchi (1978)	<ul style="list-style-type: none"> <li>• hydrostatic</li> <li>• <math>f=0, Pr=1</math></li> <li>• length of island <math>l</math></li> </ul>	$\begin{pmatrix} x_* \\ z_* \end{pmatrix} = l \begin{pmatrix} x \\ z \end{pmatrix}$ $\begin{pmatrix} u_* \\ v_* \\ w_* \end{pmatrix} = \frac{g\alpha\Delta T_*}{N} \begin{pmatrix} u \\ v \\ w \end{pmatrix}$	<ul style="list-style-type: none"> <li>• <math>l</math> for <math>\Omega &lt; 1.3</math> (heat island)</li> <li>• for <math>\Omega \gg 1</math>, determined by characteristics of internal gravity wave <math>(N/\omega_*) \sqrt{\kappa/\omega_*}</math>?</li> </ul>	value of $x$ at which $u$ becomes $1/e$ of its maximum value.	flow field is determined by a non-dimensional parameter $\Omega = \omega_* \left( \frac{l^2}{\kappa N^2} \right)^{1/3}$
Ueda (1983)	<ul style="list-style-type: none"> <li>• non-hydrostatic</li> <li>• <math>f \neq 0</math></li> <li>• <math>Pr=1</math></li> </ul>	same as Walsh (1974) except that $\begin{pmatrix} x_* \\ z_* \end{pmatrix} = \sqrt{\frac{\nu}{\omega_*}} \begin{pmatrix} x \\ z \end{pmatrix}$ .	$\left( \frac{N}{\omega_*} \right)^{0.774} \sqrt{\frac{\kappa}{\omega_*}} Pr^0$	value of $x$ at which $u$ becomes 25% of its value at $x=0$ at the level of $z=0.25$ .	horizontal scale depends little on $f$ .
Rottuno (1983)	<ul style="list-style-type: none"> <li>• hydrostatic</li> <li>• <math>f \neq 0</math></li> <li>• <math>Pr=0</math> (inviscid)</li> </ul>	/	$\frac{N}{\omega \sqrt{1-f^2}} \sqrt{\frac{\kappa}{\omega_*}} \text{ for } f < 1$ <p>(wavelength of inertia gravity wave)</p> $\frac{N}{\omega \sqrt{f^2-1}} \sqrt{\frac{\kappa}{\omega_*}} \text{ for } f > 1$	/	when $f=1$ , effect of viscosity may be important.
Niino (1987)	<ul style="list-style-type: none"> <li>• non-hydrostatic</li> <li>• <math>0 \neq f</math></li> <li>• <math>Pr=1</math></li> </ul>	$x_* = \frac{N}{\omega_*} \sqrt{\frac{\kappa}{\omega_*}} x, z_* = \sqrt{\frac{\kappa}{\omega_*}} z$ $\begin{pmatrix} u_* \\ v_* \end{pmatrix} = \frac{g\alpha\Delta T_*}{N} \begin{pmatrix} u \\ v \end{pmatrix},$ $w_* = \frac{\omega_*}{N} \frac{g\alpha\Delta T_*}{N} w$	$\frac{N}{\omega_*} \sqrt{\frac{\kappa}{\omega_*}} F(f), \text{ where}$ $0.9 < F(f) < 2.3 \text{ for } 0 < f < 2.$	value of $x$ at which $u$ becomes 0.03.	similarity solution for fixed value of $f$ .

local time rate of change term when  $Pr$  remains of the order of one. Thus, the inertial gravity wave which plays a dominant role in the inviscid dynamics must be severely modified by the presence of viscosity.

To demonstrate the importance of the effect of viscosity for all values of  $f$ , inviscid solutions for various values of  $f$  with  $Pr=0$  and  $\delta=10^{-2}$  are obtained. Fig. 11 shows the distribution of the amplitude  $|\hat{u}(x, z)|$  for  $f=0, 0.5, 0.99$  and  $1.5$ . It is seen that the horizontal wind becomes maximum at the ground because of the free-slip condition there. Furthermore, the amplitude of LSBC is much larger than that for  $Pr=1$  (see, Fig. 7). This means that, if the same definition of the horizontal dimension of LSBC is adopted, the horizontal dimension for  $Pr=0$  is much larger than that for  $Pr=1$ . As  $f$  is increased from 0, the amplitude rapidly increases and eventually becomes infinity at  $f=1$  ( $f_*= \omega_*$ ). The amplitude distribution for  $f=0.99$  well illustrates this feature. It is also noted that the contour lines

of the amplitude become nearly horizontal. These two features make the horizontal dimension of LSBC infinite as predicted by eq. (4.3). On the other hand, when  $Pr=1$  as in the present model,  $\lambda_*$  is a monotonically decreasing function of  $f$ . Especially,  $\lambda_*$  remains finite even for  $f=1$ . Thus, the suggestion by KE and Rottuno (1983) that the horizontal dimension of LSBC is determined by the inviscid dynamics does not seem to be correct.

Ueda (1983) examined the effect of  $Pr$  on the linear dynamics of LSBC. Since he used the similar scaling to Walsh (1974) (see, Table 1), however, he also had to determine experimentally the horizontal dimension of LSBC based on the solutions for several particular combinations of the external parameters. The experimental formula for the horizontal dimension  $\lambda_*$  obtained in this way was

$$\lambda_* = \left(\frac{N}{\omega_*}\right)^{0.774} \left(\frac{\nu}{\omega_*}\right)^{1/2} Pr^0 \quad (4.4)$$

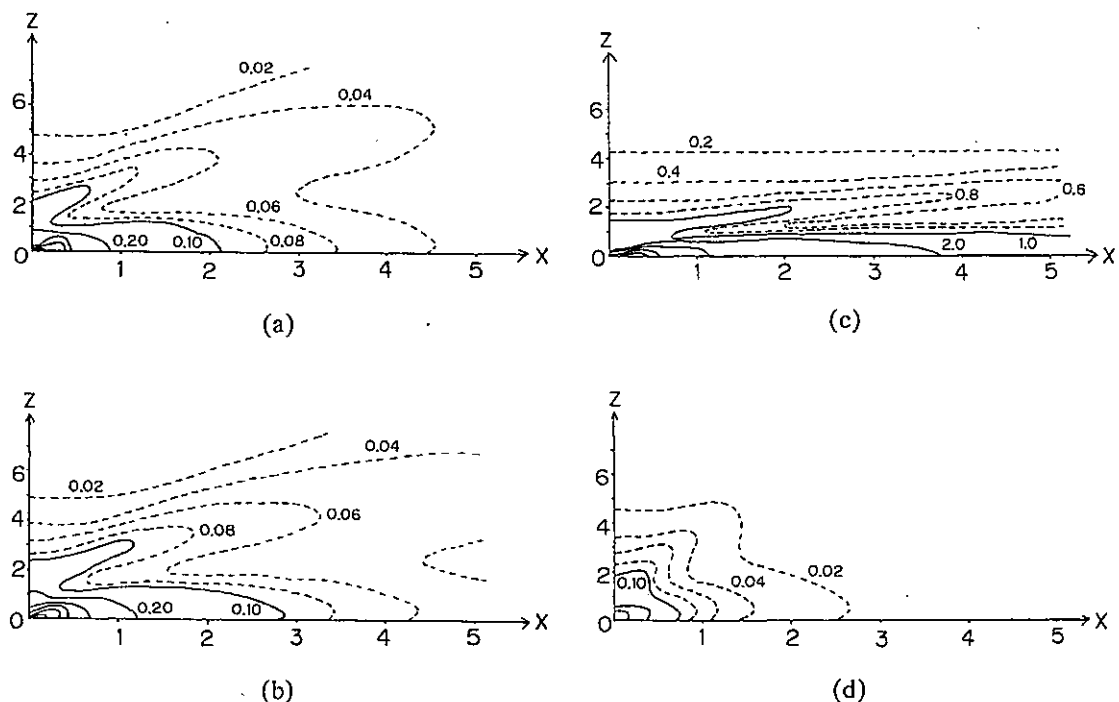


Fig. 11. Distribution of absolute value of the amplitude of the horizontal wind  $|\hat{u}(x, z)|$  for various values of  $f$  in the inviscid model ( $Pr=0$ ) ((a) $f=0$ , (b) $f=0.5$ , (c) $f=0.99$  and (d) $f=1.5$ ). Dashed contour lines are drawn for each 0.02, and solid ones for each 0.1 except for (c) in which dashed ones for each 0.2 and solid ones for each 1.0.

which is considerably different from eq. (4.1). The reason for this difference may be as follows. He defined  $\lambda_*$  as a distance from the coastline at which the horizontal wind  $u_*$  at the level of  $z_*=0.25$  ( $\nu/\omega_*$ )<sup>1/2</sup> becomes 25% of its value at  $x_*=0$ . As shown in Fig. 4, however, the vertical profile of  $|u_*|$  depends markedly on  $\delta = \omega_*/N$  because of the presence of the non-hydrostatic region. Thus the horizontal dimension defined in the above manner does not reflect the variation of  $u_*$  outside of the non-hydrostatic region but reflects that in the non-hydrostatic region. In fact, when  $\delta$  changes in the range of  $\delta < 10^{-1}$ ,  $|u_*|$  outside of the non-hydrostatic region remain unchanged as shown in Fig. 3. Thus, it does not seem to be appropriate to define  $\lambda_*$  based on  $u_*$  at some fixed level above the coastline. Rather  $\lambda_*$  should be defined by a distance from the coastline at which the suitably scaled  $u_*$  decreases to attain a particular value as is done in the present paper.

In addition to the problem described above, the expression (4.4) suggests two odd behaviors of  $\lambda_*$ . First, it does not show any dependence on the Coriolis parameter. If Fig. 6 of his paper is carefully examined,  $\lambda_*$  has a very weak dependence of  $f$  and increases with increasing  $f$ , which gives an opposite tendency to our result. The reason of this is not clear. However, the definition of  $\lambda_*$  based on  $u_*$  above the coastline seems to be responsible for producing the difference.

Secondly, eq. (4.4) suggests that  $\lambda_*$  increases with  $\nu$  and does not depend on  $\kappa$ . However, our results for  $Pr=0$  and  $Pr=1$  suggest that  $\lambda_*$  is a decreasing function of  $Pr$ . This speculation is also supported by the following physical argument: Suppose that all the external parameters except  $\nu$  is fixed and  $\nu$  is increased from 0. When  $\nu=0$ , most of the available potential energy created by the diffusion of heat from the earth's surface (except the small portion to generate internal gravity waves) can be transformed into the kinetic energy of LSBC. When  $\nu$  becomes finite, however, a part of the kinetic energy must be dissipated through the effect of the viscosity and the amplitude of the horizontal velocity must be reduced. Thus, when the Coriolis force is absent,  $\lambda_*$  seems to be given by

$$\lambda_* = \frac{N}{\omega_*} \left( \frac{\kappa}{\omega_*} \right)^{1/2} \cdot G(Pr) \tag{4.5}$$

where  $G(Pr)$  is a decreasing function of  $Pr$ . The difference between (4.4) and (4.5) again seems to be caused by the difference of the definition of  $\lambda_*$ . It is clear from the foregoing discussion, however, that the appropriate horizontal dimension is not given by (4.4) but by (4.5).

#### 4.2 LSBC over an island of finite width

As mentioned in the introduction, KE considered LSBC over an island whose width is  $l$  for  $f=0$ ,  $\delta=0$  and  $Pr=1$ . They showed that the flow field was described by a single non-dimensional frequency  $\Omega$  defined by  $\Omega = l^{2/3} \omega_*/N^{2/3} \kappa^{1/3}$ . Especially, when  $\Omega < 1.3$ , the flow structure is similar to that of the steady heat island. This criterion may be rewritten as

$$l/L < 1.5 \tag{4.6}$$

in terms of the non-dimensional width of the island,  $l/L$ , where  $L = (N/\omega_*)(\kappa/\omega_*)^{1/2}$ . Since  $L$  is proportional to the horizontal dimension of LSBC,  $\lambda_*$  and is equal to  $0.44 \lambda_*$ , eq. (4.6) may be rewritten as

$$l/\lambda_* < 0.65. \tag{4.7}$$

Now, the physical meaning of the criterion becomes evident. If the width of the island is sufficiently small compared with the horizontal dimension of LSBC, the flow fields are similar to those of the steady convection. If  $l$  is sufficiently larger than  $\lambda_*$ , on the other hand, well-defined LSBCs develop separately over the two coastlines of the island.

For typical atmospheric conditions,  $\lambda_*$  is about 60km. Thus, eq. (4.7) suggests that the flow fields around an island whose width is sufficiently smaller than 40km are similar to those of the steady heat island. It has been shown by Kimura (1975) that the horizontal and vertical dimensions of the steady heat island are given by  $l$  and  $(\kappa l^2/N^2)^{1/5}$ , respectively.

#### 4.3 Some miscellaneous problems

##### a) Effects of general wind

Effects of a uniform general wind on LSBC have been discussed by Walsh (1974) and Ueda (1983). Since the alongshore component of the general wind does not affect LSBC within the framework of a linear theory, only the onshore or offshore component needs to be considered. When a uniform general wind  $U_*$  perpendicular to the coastline is present, the local derivatives with respect to time in eqs. (2.11) – (2.14) must be replaced by  $\partial/\partial t + U(\partial/\partial x)$ , where  $U$  is a Froude number defined by

$$U = \frac{U_*}{N(\kappa_*/\omega_*)^{1/2}} \quad (4.6)$$

Thus, when the Coriolis force is absent and  $Pr=1$ , LSBC in the uniform general wind is a function of only  $U$ . For typical atmospheric conditions  $N(\kappa_*/\omega_*)^{1/2} \sim 3\text{m}\cdot\text{s}^{-1}$ . Since the effects of the general wind is expected to become significant for  $U > 1$ , a general wind of  $3\text{m}\cdot\text{s}^{-1}$  or more would affect the dynamics of LSBC considerably.

In his study of the effects of the general wind on LSBC, Walsh (1974) used a non-dimensional general wind  $U_{nd}$  defined by

$$U_{nd} = \frac{U_*}{\omega_*(\kappa_*/\omega_*)^{1/2}} = \delta^{-1}U. \quad (4.7)$$

If his results are expressed in terms of  $U$ , they become to include the results for more general cases except in the immediate neighbourhood of the coastline (e.g., Figs. 6 and 9 of his paper). Ueda (1983) used another nondimensional general wind  $\tilde{U}_{nd}$  defined by

$$\tilde{U}_{nd} = \frac{U_*\nu}{(\kappa_*/\omega_*)^{1/2}} = \delta^{-1}Pr^{1/2}U. \quad (4.8)$$

In his Figs. 1, 2 and 3,  $Pr$  is unity. Therefore, if his results are expressed in terms of  $U$ , they also become to include those for more general cases.

It is noteworthy that, when the general wind is present, eqs. (2.17) and (2.18) are modified to

$$\left[ \left( i - \delta^2 \frac{\partial^2}{\partial x^2} - \frac{\partial^2}{\partial z^2} + U \frac{\partial}{\partial x} \right)^2 \left( \delta^2 \frac{\partial^2}{\partial x^2} + \frac{\partial^2}{\partial z^2} \right) + f^2 \frac{\partial^2}{\partial z^2} + \frac{\partial^2}{\partial x^2} \right]$$

$$\cdot \left( i - \delta^2 \frac{\partial^2}{\partial x^2} - \frac{\partial^2}{\partial z^2} + U \frac{\partial}{\partial x} \right) T = 0 \quad (4.9)$$

and

$$\left[ \left( i + U \frac{\partial}{\partial x} - \frac{\partial^2}{\partial z^2} \right)^2 \frac{\partial^2}{\partial z^2} + f^2 \frac{\partial^2}{\partial z^2} + \frac{\partial^2}{\partial x^2} \right] \cdot \left( i + U \frac{\partial}{\partial x} - \frac{\partial^2}{\partial z^2} \right) T = 0. \quad (4.10)$$

The similar argument as in Section 2.2 suggests that the non-hydrostatic terms become important for  $x < O(\delta)$  and  $z < O(1)$  because of the  $U(\partial/\partial x)$  term. Since  $\delta$  is a small quantity for the usual atmospheric conditions, however, the overall feature of the solution is expected to depend on only  $U$  but not on  $\delta$ .

#### b) Vertical heat flux

The vertical flux associated with LSBC was studied by Walsh (1974). He considered two vertical fluxes, the time-averaged vertical heat flux  $F_*(x_*)$  defined by

$$F_*(x_*) = \frac{\rho c_p \omega_*}{2\pi} \int_0^{2\pi/\omega_*} dt_* \int_{-x_*}^{x_*} w_* T_*' dx_*$$

and the horizontally integrated, time-averaged vertical heat flux  $F_{o*}$  defined by  $F_*(\infty)$ , where  $\rho$  is the mean density and  $c_p$  the specific heat. In the present scaling,

$$F_*(x_*) = \frac{\rho c_p}{2\pi} \cdot \frac{g\alpha(\Delta T)^2}{N} \cdot (\kappa/\omega_*)^{1/2} \int_0^{2\pi} dt \int_{-x}^x wT dx. \quad (4.11)$$

Thus,  $F_*$  and  $F_{o*}$  are scaled by

$$\rho c_p [g\alpha(\Delta T)^2/N] (\kappa/\omega_*)^{1/2}, \quad (4.12)$$

which shows that the vertical heat fluxes are inversely proportional to  $N$  and proportional to the diffusion length.

In his explanation of Fig. 8, Walsh (1974) mentioned that "the flux in a case of a uniform stability is approximately tripled when  $N^2$  is increased by an order of magnitude." This is nothing but a reflection of the dependence of the heat fluxes on  $N$  in eq. (4.12). It is likely that the two curves for  $N^2 = 10^{-3}$  and  $10^{-4}$  in his Fig. 8 would collapse to a single universal

curve if  $F_*$  is scaled according to (2.9). Similarly, his Figs. 7 and 9 would include the results for more general cases after the scaling is changed.

It is of interest whether the heat fluxes near the ground depend on the value of  $\delta$  or not, since the non-hydrostatic layer exists for  $z < O(\delta^{1/2})$  near the coastline. In the non-hydrostatic layer,  $w \sim O(\delta^{-1})$ ,  $x \sim O(\delta^{3/2})$  and  $T \sim O(1)$ . Thus, the contribution of the vertical heat fluxes in the non-hydrostatic layer to the total vertical heat fluxes are of the order of  $\delta^{1/2}$  in the non-dimensional unit. This means that the vertical heat fluxes depend little on the value of  $\delta$  and are subject to the scaling (4.12). The vertical heat flux (or equivalently the buoyancy production term in the energy balance equation) is the only source of the kinetic energy of LSBC. That the non-hydrostatic region contributes very little to the vertical heat flux is consistent with the fact that the flow fields outside of the non-hydrostatic layer does not depend on the value of  $\delta$ .

*c) Asymptotic behavior of LSBC for large non-dimensional Coriolis parameter*

In this subsection, we shall consider the asymptotic behavior of LSBC when the non-dimensional Coriolis parameter  $f$  is large. This is equivalent to considering the case in which the forcing frequency  $\omega_*$  becomes small for a fixed value of the Coriolis parameter  $f_*$ , or  $f_*$  becomes large for a fixed value of  $\omega_*$ . This latter case does not occur in nature, but can be realized in a laboratory experiment. For large values of  $f$ , the time rate of change terms in eqs. (2.11) and (2.12) becomes much smaller than the Coriolis terms and may be neglected. This suggests that the correct scaling of variables for this case is:

$$\begin{aligned} t_* &= f_*^{-1} t, & x_* &= \frac{N}{f_*} \left(\frac{\nu}{f_*}\right)^{1/2} Pr^{1/2} x, \\ z_* &= \left(\frac{\nu}{f_*}\right)^{1/2} z, & u_* &= \frac{g\alpha\Delta T_*}{N} Pr^{-1/2} u, \\ w_* &= \frac{f_*}{N} \frac{g\alpha\Delta T_*}{N} Pr^{-1} w, \\ p_* &= g\alpha\Delta T_* \left(\frac{\nu}{f_*}\right)^{1/2} p, \\ T'_* &= \Delta T_* \cdot T, & \omega_* &= f_* \cdot \omega. \end{aligned} \tag{4.13}$$

When the above scaling is introduced, the governing equations and the boundary conditions may be approximated as

$$-v = -\frac{\partial p}{\partial x} + \frac{\partial^2 u}{\partial z^2}, \tag{4.14}$$

$$u = \frac{\partial^2 v}{\partial z^2}, \tag{4.15}$$

$$0 = -\frac{\partial p}{\partial z} + T, \tag{4.16}$$

$$w = \frac{\partial^2 T}{\partial z^2}, \tag{4.17}$$

and

$$u = v = w = 0 \text{ and}$$

$$T = \begin{cases} \cos \omega t & (x > 0) \\ 0 & (x < 0) \end{cases} \text{ at } z = 0, \tag{4.18}$$

where the hydrostatic approximation is made and the continuity equation is given by (2.8).

An inspection of eqs. (4.14) – (4.18) and (2.8) reveals that this problem has a similarity solution. For example, the similarity solution for  $u$  is given by

$$u = u(x, z) \cdot \cos \omega t.$$

In dimensional units,

$$\begin{aligned} u_* &= \frac{g\alpha\Delta T_*}{N} \cdot (\kappa/\nu)^{1/2} \cdot u \left( \frac{f_*}{N} \cdot (f_*/\nu)^{1/2} \right. \\ &\quad \left. \cdot (\kappa/\nu)^{1/2} x_*, (f_*/\nu)^{1/2} z_* \right) \cos \omega_* t_* \end{aligned} \tag{4.19}$$

Thus, the horizontal and the vertical dimensions of LSBC for large  $f$  are of the order of  $(N/f_*) \cdot (f_*/\nu)^{-1/2} \cdot (\kappa/\nu)^{1/2}$  and  $(f_*/\nu)^{-1/2}$ , respectively. Now one might be tempted to apply these results to the seasonal wind circulation in which the forcing frequency  $\omega_*$  is  $2\pi \text{ year}^{-1}$ . For the usual atmospheric conditions, the dimensions derived above correspond to  $20(\sin\phi)^{-3/2} \text{ km}$  and  $300(\sin\phi)^{-1/2} \text{ m}$ , respectively. In the real atmosphere, however, the seasonal wind circulations seem to have much larger horizontal dimension (at least in the midlatitudes). This is probably because the seasonal wind circulations in the real atmo-

sphere are driven by the thermal forcings not only at the ground but also in the free atmosphere.

The scaling (4.13) suggests that, for  $f_* \gg \omega_*$ ,  $\lambda_*$  is of the order of  $(N/f_*) \cdot (f_*/\nu)^{-1/2} \cdot (\kappa/\nu)^{1/2}$ . For  $Pr=1$ , this means that  $F(f)$  is proportional to  $f^{-3/2}$  (see, eq. (2.16)). Thus, if the scaling (2.9) would have been used instead of (4.13), the horizontal scale of LSBC changes like  $f^{-3/2}$  as  $f$  is increased (cf. Figs. 7 and 9).

Including the effects of general wind, Ueda (1983) considered the solution of eqs. (4.14) – (4.18) and (2.8) under a different scaling of variables. His Figs. 1, 2 and 3 which are obtained for a special combination of the external parameters will become to include the results for more general cases if the scaling is changed to the present one and the general wind  $U^*$  is scaled by  $N(\nu/f_*)^{1/2}$  (cf., § 4.3(a)).

#### 4.4 Effects of non-linearity

In order to examine the effects of non-linearity on LSBC, an initial value problem given by eqs. (2.4) ~ (2.8) and the boundary conditions (2.10) are solved numerically for the case of  $\delta=0$ ,  $f=0$  and  $Pr=1$ . The size of the domain used for the numerical computation is 25.6 and 9.6 in the horizontal and vertical directions. Cyclic boundary conditions are assumed at the lateral boundaries. All the velocity components vanish at the vertical boundaries. The temperature perturbation is fixed to zero at the upper boundary, while at the lower boundary it is given by

$$T = [1 + \tanh(x/d)] \sin(t), \quad (4.8)$$

where  $d$  gives the width of the transition zone in which the temperature perturbation smoothly changes from its value at the sea surface to that at the land surface. Throughout the present calculation,  $d=0.2$  is adopted.

The finite difference scheme of the advection terms is the same as Yoshizaki's (1985) which conserves total energy and total enstrophy. The grid intervals in the  $x$ - and  $z$ -directions are equal and  $\Delta x = \Delta z = 0.2$ . As for the time integration, the leap-frog scheme with the time interval  $\Delta t = \pi/100$  is used.

The computation is started from the basic

state by introducing the temperature perturbation given by (4.8) at the lower boundary. It takes about seven days for the flow fields to become steady in the sense that the fractional change of the total kinetic energy in the whole domain from a certain time to the same time of the following day becomes less than 0.5%.

The computations are made for several values of  $\epsilon$ . In the following, however, we will show the results for  $\epsilon=0$ , which corresponds to the linear theory, and for  $\epsilon=2$ , which is the largest value of  $\epsilon$  adopted in the computations. Although we have attempted to make the computation for  $\epsilon$  larger than 2, we have not succeeded because of a numerical instability. This may be due to the following reason: During the daytime, the vertical gradient of the temperature perturbation becomes negative near the land surface. If a Rayleigh number is defined near the surface, based on the diffusion length  $(\kappa/\omega_*)^{1/2}$  and the total temperature difference over this length, it may be written as

$$Ra = g\alpha[\Delta T - \Gamma(\kappa/\omega_*)^{1/2}](\kappa/\omega_*)^{3/2}/\kappa^2 \\ = (\epsilon - 1)\delta^{-2}, \quad (4.9)$$

where  $Pr=1$  is assumed. Since  $\delta$  is usually a small quantity,  $Ra$  can easily exceed the critical value for the thermal instability only if  $\epsilon$  is sufficiently larger than 1. Since the horizontal wavelength of the fastest growing mode of the thermal instability is likely to be smaller than the grid interval  $\Delta x$ , perturbations which have the wavelength of  $2\Delta x$  are expected to dominate the flow fields with time in the numerical model. Thus, the numerical instability is eventually generated. It is noted, however, that in our model the eddy diffusivity  $\kappa$  and eddy kinematic viscosity  $\nu$  are assumed to express the effects of mixing due to subgrid motions including those generated by the thermal instability. Thus, it may not be meaningful to consider cases in which  $\epsilon$  is much larger than 1.

Fig. 12 shows time evolutions of the horizontal velocity  $u$  for  $\epsilon=0$  and  $\epsilon=2$  during the tenth day from the start of the computation. It is seen that the evolutions for  $\epsilon=0$  and  $\epsilon=2$  are considerably similar. However, several differences between them are also found: The distribution of  $u$  for  $\epsilon=0$  is symmetric with respect to  $x=0$ ,

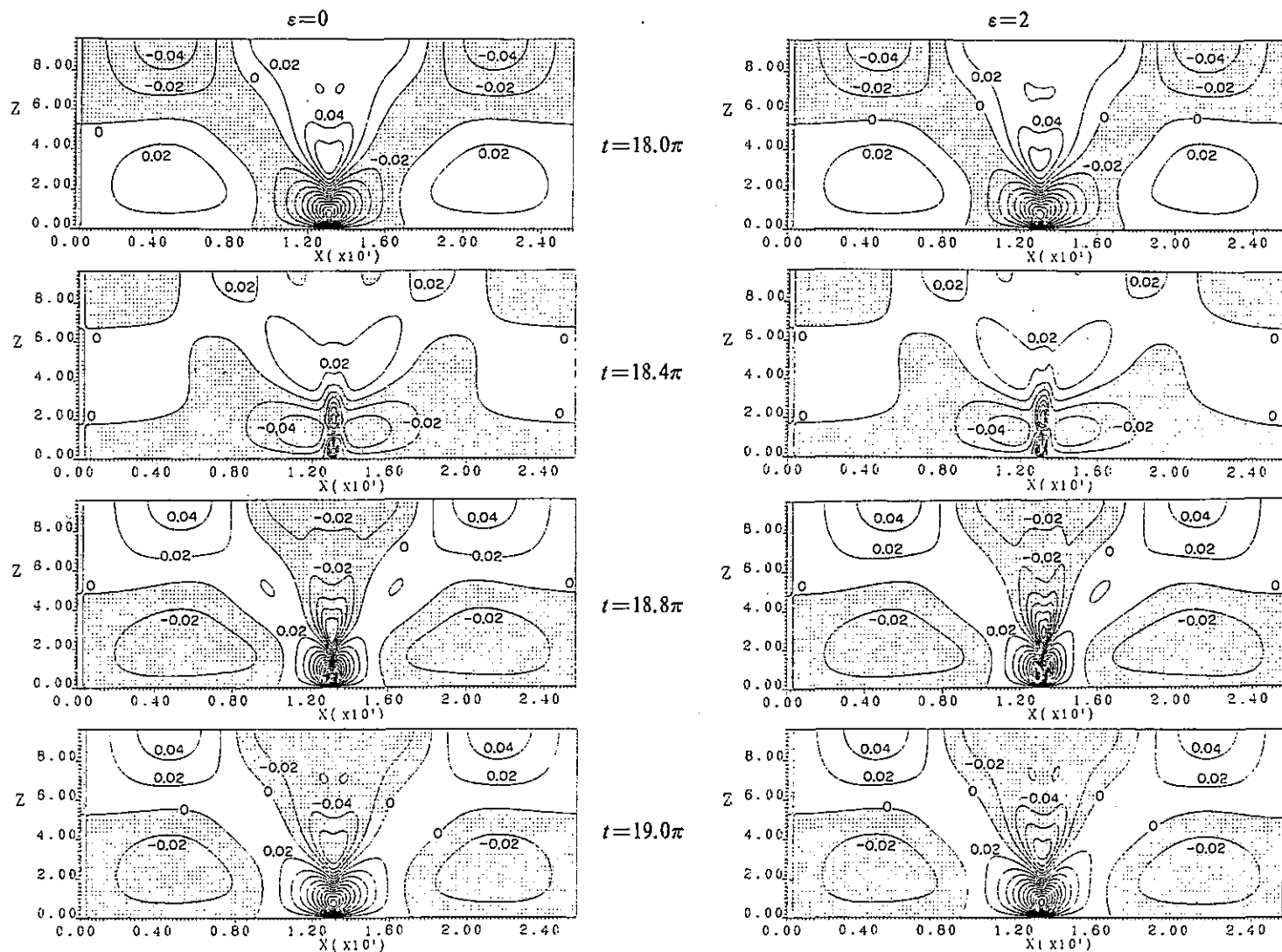


Fig. 12. Time evolutions of the horizontal velocity  $u$  for  $\varepsilon=0$  and 2 obtained by the numerical model. Contour lines are drawn for each 0.02.

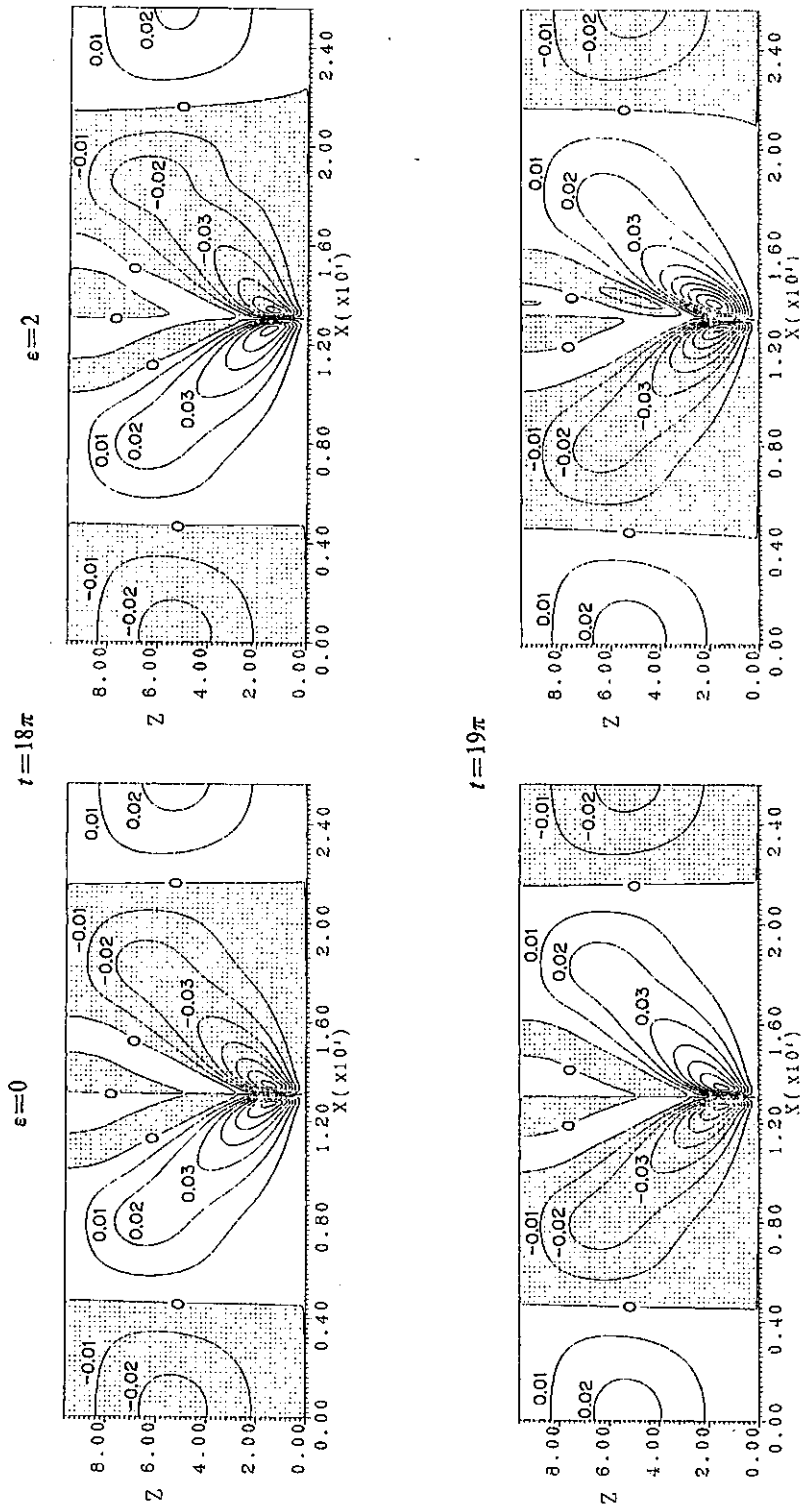


Fig. 13. Same as Fig. 12 except for the vertical velocity  $w$ . Contour lines are drawn for each 0.01.

and its time evolution is similar to the one as shown in Fig. 10. The distribution of  $u$  for  $\varepsilon=2$ , however, is not symmetric with respect to  $x=0$ . At  $t=18\pi$  when the temperature perturbation at the land surface changes its sign from negative to positive, the depth of the land breeze over the sea is 3.0 and is larger than that over the land, 2.85, where the depth of the breeze is defined by the maximum height attained by the contour line of  $u=0.02$ . At  $t=19\pi$ , on the other hand, the depth of the sea breeze over the land is 3.4 and is larger than that over the sea, 3.1. In the linear model ( $\varepsilon=0$ ), all the depths considered above are equal to 3.0.

The difference in the depths of the breezes for  $\varepsilon=2$  reflects the difference in their intensities and may be explained in terms of the scaling in the linear theory. As eq. (2.10) shows, the horizontal velocity  $u_*$  is scaled by  $g\alpha\Delta T/N$ , where  $N$  is the Brunt-Väisälä frequency corresponding to the basic stratification. In the non-linear model, however, the basic stratification is modified by the temperature perturbation. Thus, the effective value of the Brunt-Väisälä frequency,  $N_e$ , over the land in the daytime becomes smaller than  $N$  and larger in the nighttime. This fact and eq. (2.10) suggest that the sea breeze is stronger than the land breeze even in the model in which the eddy diffusivities are constant both in time and space. The effect of the temperature stratification on the relative intensities of the land and sea breezes has been found by Mak and Walsh (1976) based on a linear theory in which the temperature stratification was a periodic function of time.

Effects of the variation of  $N_e$  are also reflected in the behaviour of the vertical velocity. Fig. 13 shows the distributions of the vertical velocity for  $t=18\pi$  and  $19\pi$  and for  $\varepsilon=0$  and  $\varepsilon=2$ . In the linear model, the vertical velocity is anti-symmetric with respect to  $x=0$ . In the non-linear model, however, it is not. At  $t=18\pi$  when  $N_e$  over the land is large, the vertical velocity over the land is slightly weaker than that in the linear model. At  $t=19\pi$  when  $N_e$  over the land is small, on the other hand, the vertical velocity over the land is larger than that over the sea, and both are larger than that in the linear model.

As to the non-dimensional horizontal di-

mension of the sea breeze,  $\lambda$ , the linear model gives  $\varepsilon=2.10^4$ , while the non-linear model ( $\varepsilon=2$ ) gives  $\lambda=2.15$ . Thus,  $\lambda$  seems to be a weakly increasing function of  $\varepsilon$ . Since  $\varepsilon$  can be considered as a ratio of the advection velocity to the group velocity of the hydrostatic internal gravity wave whose vertical scale and frequency are  $(\kappa/\omega_*)^{1/2}$  and  $\omega_*$ , respectively, it is expected that, when  $\varepsilon$  is sufficiently larger than unity, the penetration velocity of the sea breeze into inland is determined by the advection velocity. This means that the front of the sea breeze bears the nature of a gravity current as suggested from observations (e.g., Simpson *et al.*, 1977) and laboratory experiments (e.g., Mitsumoto *et al.*, 1983). It would be interesting to see the dependence of  $\lambda$  on  $\varepsilon$  for larger values of  $\varepsilon$ . However, the numerical instability and the assumption of the constant eddy diffusivity and constant eddy kinematic viscosity have prevented the computations for  $\varepsilon>2$  as described above.

## 5. Summary and conclusions

The linear theory of land and sea breeze circulation is developed to clarify the physical process which determines the horizontal dimension of LSBC. It is found that, after suitable scaling of variables and under hydrostatic approximation, a similarity solution exists when the Coriolis force is absent and the eddy Prandtl number is one. Even if the non-hydrostatic effects are considered, the solution remains valid outside the tiny region right above the coastline where the hydrostatic approximation breaks down. The existence of the similarity solution has not been noticed in the previous studies Walsh (1974), Kimura and Eguchi (1978), Ueda (1983) and Rottuno (1983), whose results are critically discussed in the light of the present study. The horizontal and vertical dimensions of LSBC are scaled by  $N\kappa^{1/2}\omega_*^{-3/2}$  and  $\kappa^{1/2}\omega_*^{-1/2}$ , respectively, and the horizontal and vertical velocities by  $g\alpha\Delta T/N$  and  $g\alpha\Delta T \cdot \omega_*/N^2$ , respectively.

When the Coriolis force is present, the solution depends on the non-dimensional Coriolis

<sup>4)</sup> This value is slightly smaller than the theoretical value, 2.2.

parameter  $f = f_*/\omega_*$ . Especially, the horizontal dimension  $\lambda_*$  of LSBC is given by  $\lambda_* = N\kappa^{1/2}\omega_*^{-3/2} F(f)$ , where  $F(f)$  is a function of  $f$ .  $F$  remains almost constant ( $\sim 2.1$ ) for  $f < 1$  (latitude less than  $30^\circ$ ), but decreases rapidly with increasing  $f$  for  $f > 1$ .  $F$  becomes 0.9 for  $f = 2$  which corresponds to the poles. These results suggest that the effect of the Coriolis force is not important for LSBC for latitudes less than  $30^\circ$ . It would be of interest to compare the present results with observations at various latitudes if available.

The effect of increasing the eddy Prandtl number  $Pr = \nu/\kappa$  is argued to weaken LSBC and therefore to decrease the horizontal dimension of LSBC.

The effect of the nonlinearity is also examined by a nonlinear numerical model. It is found that the nonlinearity breaks down several symmetries of LSBC which are present in the linear model. These features are explained in terms of variation of the effective temperature stratification. It is also found that, within the degree of nonlinearity considered in this paper, the effect of nonlinearity increases the horizontal dimension of sea breeze circulation only slightly. Unfortunately, the assumption of constant eddy diffusivity and eddy kinematic viscosity prevented us from studying the effect of strong nonlinearity on the flow field. However, it should be remembered that the same assumption has simplified the problem considerably and enabled us to obtain a physical insight leading to the various important deductions described above.

#### Acknowledgements

The author would like to express his hearty thanks to Profs. R. Kimura and T. Asai and Messrs. S. Mitsumoto and H. Kondo for fruitful discussions. He is also grateful to Mr. H. Uemura, Dr. T. Hanafusa, Miss M. Kato, and Mr. T.

Fujitani for invaluable supports and encouragements, Dr. M. Murakami for collaboration in constructing the nonlinear numerical model used in the present study, and two anonymous referees for invaluable comments. Thanks are extended to Dr. Y. Ishikawa and Miss Y. Miyauchi for assistance in wordprocessing, to Miss N. Ishii for drawing figures and to Dr. J. Simpson for correcting english expressions. This work was financially supported in part by Research Project, Grant-in-Aid for Scientific Research of the Ministry of Education, Project Number 61460047. The numerical computations were performed by the HITAC S-810 computer at the Meteorological Research Institute Computer Centre.

#### References

- Jeffreys, H., 1922: On the dynamics of wind. *Quart. J. Roy. Meteor. Soc.*, **48**, 29-46.
- Kimura, R., 1975: Dynamics of steady convections over heat and cool islands. *J. Meteor. Soc. Japan*, **53**, 440-457.
- Kimura, R. and T. Eguchi, 1978: On dynamical processes of sea- and land-breeze circulation. *J. Meteor. Soc. Japan*, **56**, 67-85.
- Mak, M.K. and J.E. Walsh, 1976: On the relative intensities of sea and land breezes. *J. Atmos. Sci.*, **33**, 242-251.
- Mitsumoto, S., H. Ueda and H. Ozoe, 1983: A laboratory experiment on the dynamics of the land and sea breeze. *J. Atmos. Sci.*, **40**, 1228-1240.
- Rottuno, R., 1983: On the linear theory of the land and sea breeze. *J. Atmos. Sci.*, **40**, 1999-2009.
- Simpson, J.E., D.A. Mansfield and J.R. Milford, 1977: Inland penetration of sea-breeze fronts. *Quart. J. Roy. Met. Soc.*, **103**, 47-76.
- Ueda, H., 1983: Effects of external parameters on the flow field in the coastal region - a linear model. *J. Appl. Meteor.*, **22**, 312-321.
- Walsh, J.E., 1974: Sea breeze theory and applications. *J. Atmos. Sci.*, **31**, 2012-2026.
- Yoshizaki, M., 1985: A new second-order finite-difference form of three-dimensional momentum equations in the anelastic system. *J. Meteor. Soc. Japan*, **63**, 397-404.

## 海陸風循環の線形論\*

新野 宏

(気象研究所)

海陸風循環の性質を線形論で調べた。静水圧近似のもとでは、コリオリ力がなければ、海陸風循環の線形論は相似解を持つ。相似解に現れる各変数のスケーリングから、海陸風の水平・鉛直スケールはそれぞれ  $N\kappa^{1/2}\omega_*^{-3/2}$ ,  $\kappa^{1/2}\omega_*^{-1/2}$  で、水平・鉛直速度のスケールは  $g\alpha\Delta T/N$ ,  $g\alpha\Delta T\omega_*/N^2$  で、圧力のスケールは  $g\alpha\Delta T\kappa^{1/2}\omega_*^{-1/2}$  で与えられることがわかった。ここで、 $\omega_*$  と  $\Delta T$  は地表面で与える温度の周期的時間変化の振動数と振幅、 $N$  は基本場の浮力振動数、 $\kappa$  は渦温度伝導率、 $g$  は重力加速度、 $\alpha$  は体膨張率である。渦プラントル数は1を仮定した。

海岸線の近くの非常に小さな領域では静水圧近似が成り立たないため、相似解も成り立たなくなる。この非静水圧領域の水平・鉛直スケールは共に  $(\kappa/N)^{1/2}$  のオーダーであり、ここでは鉛直速度が水平速度と同じオーダーになる。しかし、この領域の外側では相似解は至るところで有効である。

コリオリ力が存在するとき、非静水圧領域の外側の解は無次元コリオリ係数  $f=f_*/\omega_*$  のみに依存する。海陸風循環の水平スケール  $\lambda_*$  を、海風の無次元流速が0.03に減少する海岸線からの距離で定義すると、 $\lambda_*=N\kappa^{1/2}\omega_*^{-3/2}\cdot F(f)$  で与えられる。ここで  $F(f)$  は  $f$  の普遍関数である。 $F$  は  $f < 1$  すなわち緯度が30度以下のときにはほぼ一定 ( $\sim 2.1$ ) にとどまるが、 $f > 1$  になると  $f$  と共に急激に減少し、南極・北極にあたる  $f = 2$  に対しては0.9となる。

渦プラントル数及び非線形過程の流れに及ぼす効果についても議論する。

\* この論文は1986年7月、大気力学に関する京都国際セミナーにおいて発表したものである。